

Supplementary Information

Aperiodic “Bricks and Mortar” Mesophase: a New Equilibrium State of Soft Matter and Application as a Stiff Thermoplastic Elastomer

Weichao Shi[†], Andrew Hamilton[†], Kris T. Delaney[†], Glenn H. Fredrickson^{†,‡,*}, Edward J. Kramer^{†,‡,§}

[†]Materials Research Laboratory, [‡]Department of Chemical Engineering, [§]Department of Materials, University of California at Santa Barbara, California, United States, 93106

Christos Ntaras[#] and Apostolos Avgeropoulos^{#,*}

[#]Department of Materials Science and Engineering, University of Ioannina, University Campus, Ioannina, Greece 45110

Nathaniel A. Lynd^{⊥,¶}

[⊥]McKetta Department of Chemical Engineering, University of Texas at Austin, Austin, TX 78712.

[¶]Materials Sciences Division, Lawrence Berkeley National Laboratory, Berkeley, CA 94720

Quentin Demassieux^{||}, Costantino Creton^{||}

^{||}Laboratory of Soft Matter Science and Engineering, ESPCI Paristech-CNRS-UPMC, 10 rue Vauquelin, 75005 Paris, France

Content:

Part A: Samples used and molecular characterization

Part B: Full TEM diagram for miktoarm copolymer ($f_{PS}=0.37$) and hPS

Part C: 10-day annealing experiment

Part D: SAXS curves

Part E: Bricks-and-mortar structure in miktoarm ($f_{PS}=0.48$) and hPS blends

Part F: Phase diagram of miktoarm and hPS by SCFT

Part G: Monotonic and step-cycle tensile testing results

Part H: Monotonic and modulus at different hPS fractions

Part I: Scattering curves for the tensile-SAXS experiment at different strains

Part A: Samples used and molecular characterization

Table S1. Molecular parameters for miktoarm block copolymers.

Sample	\overline{M}_n PS (kg/mol)	\overline{M}_n PI (kg/mol)	\overline{M}_n PS' (kg/mol)	\overline{M}_n total ^a (kg/mol)	<i>PDI</i> total	\overline{M}_w total (kg/mol)	%wt _{PS} (¹ H-NMR)	<i>f</i> _{PS}
<i>S(IS')</i> ₃	80.5	56.0	11.0	281.5	1.04	293	0.41	0.37
<i>S(IS')</i> ₃	81.0	31.5	10.5	207.0	1.03	213	0.52	0.48

^a the total molecular weight is calculated by $\overline{M}_{n\text{total}} = (\overline{M}_n)_{PS} + 3(\overline{M}_n)_{PS'-b-PI}$.

Table S2. Molecular characterization for PS homopolymers.

Sample	\overline{M}_n (kg/mol) ^a	\overline{M}_w (kg/mol) ^a	PDI ^a	\overline{M}_n (kg/mol) ^b	\overline{M}_w (kg/mol) ^b	PDI ^b
1	4.7	5.4	1.14	5.0	6.0	1.20
2	10.5	11.4	1.09	9.9	11.0	1.11
3	21.0	21.8	1.04	20.8	22.3	1.07
4	44.0	45.8	1.04	44.6	48.1	1.08
5	80.5	85.0	1.06	79.5	84.2	1.06

^a Molecular parameters were given by the vendor (Polymer Source); ^b Molecular parameters obtained by GPC in our own lab, referencing to standard PS homopolymer in chloroform.

Part B: Full TEM diagram for miktoarm copolymer ($f_{PS}=0.37$) and hPS

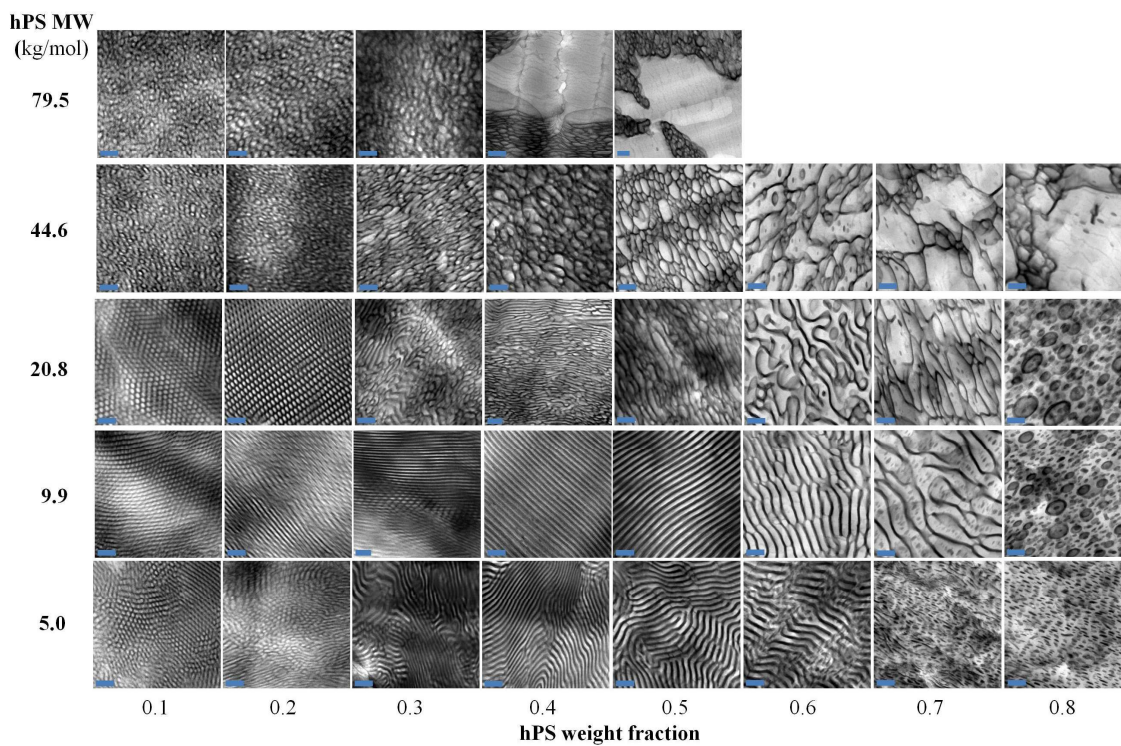


Figure S1. The full TEM diagram for miktoarm ($f_{PS}=0.37$) and hPS blends, supplemental to Figure 2 in the manuscript. The scale bars are 200 nm in all images.

Part C: 10-day annealing experiment

1. 10 day annealing (hPS 20.8 kg/mol)

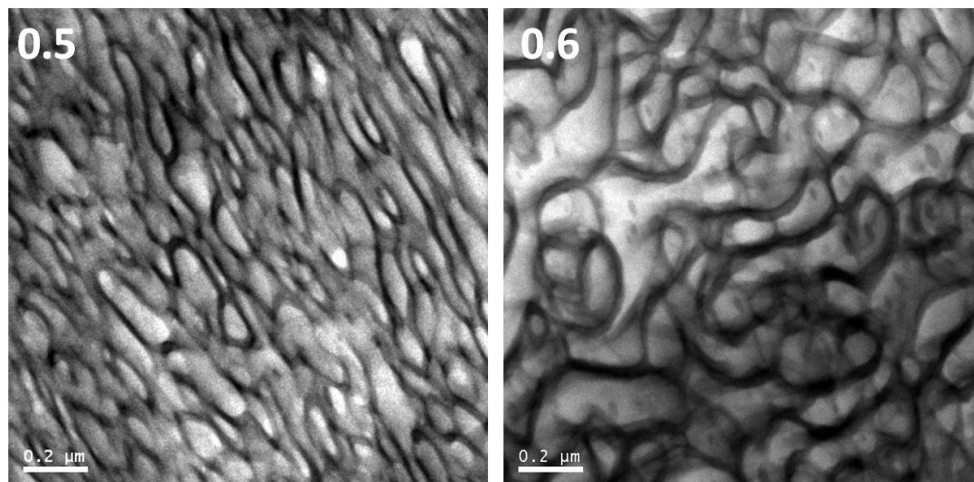


Figure S2. TEM images for miktoarm ($f_{PS}=0.37$) and hPS (20.8 kg/mol) blends with 50 wt% and 60 wt% of hPS, respectively. The sample was annealed in high vacuum oven at ~ 150 °C for 10 days.

2. 10-day annealing (hPS 44.6 kg/mol)

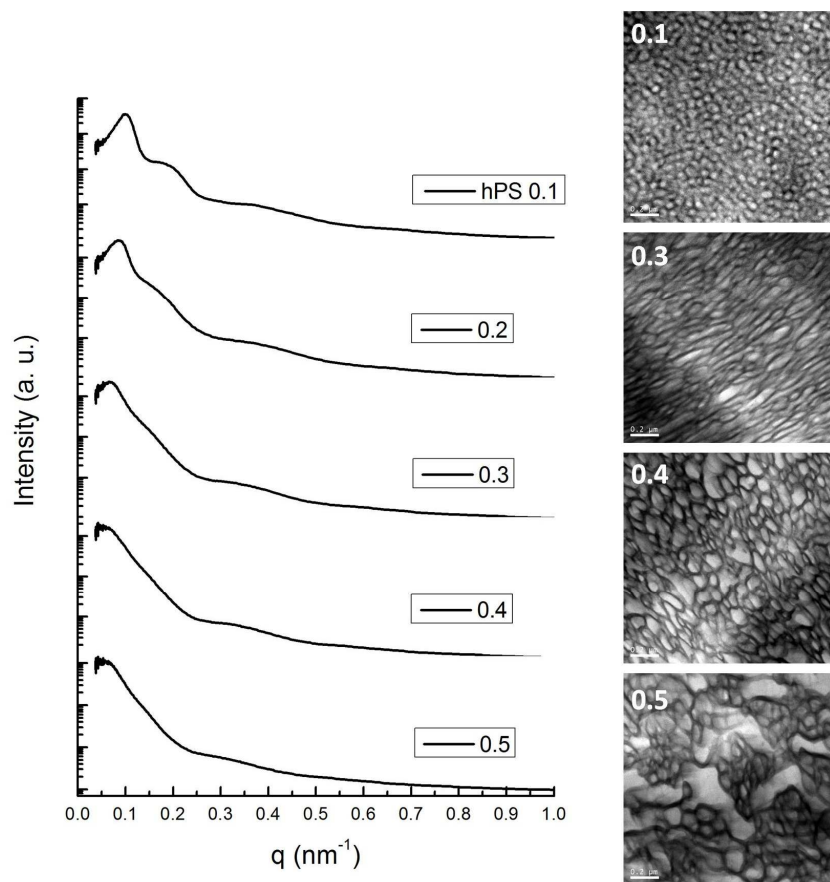


Figure S3. SAXS curves and TEM images for miktoarm ($f_{PS}=0.37$) and hPS (44.6 kg/mol) blends with 10~50 wt% of hPS, respectively. The sample was annealed in a high vacuum oven at ~ 150 °C for 10 days. The scale bars corresponds to 200 nm.

Part D: SAXS curves

1. hPS: 5.0 kg/mol

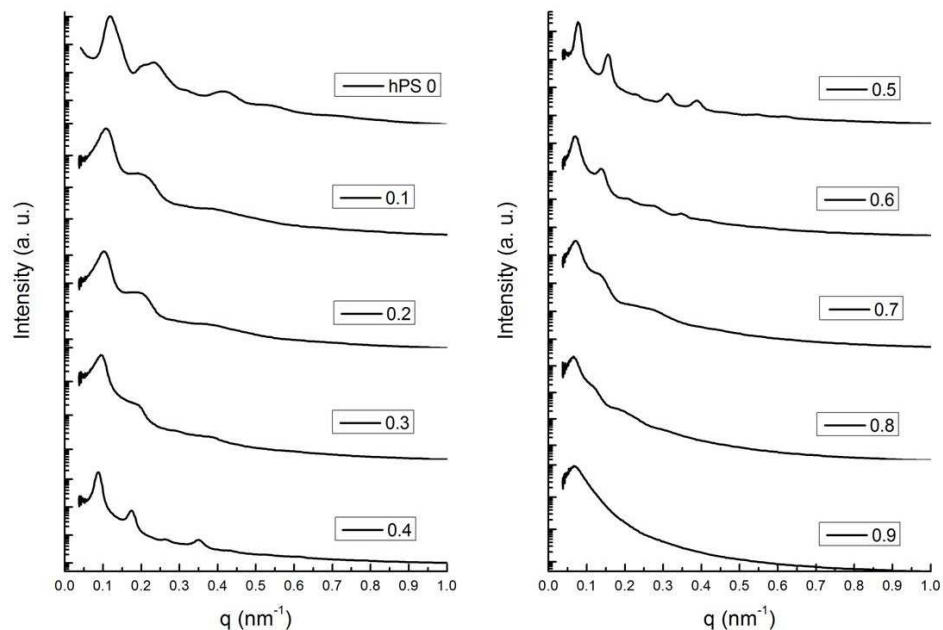


Figure S4. SAXS curves for miktoarm ($f_{PS}=0.37$) and hPS (5.0 kg/mol) blends. The numbers on each curve represent the wt fraction of hPS in each blend

2. hPS: 9.9 kg/mol

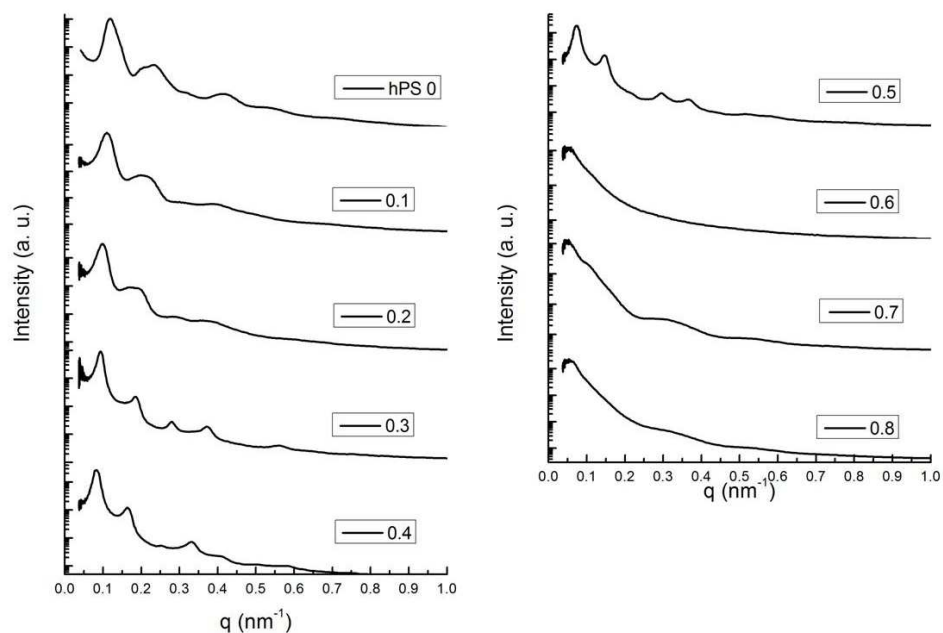


Figure S5. SAXS curves for miktoarm ($f_{PS}=0.37$) and hPS (9.9 kg/mol) blends. The

numbers on each curve represent the wt fraction of hPS in each blend.

3. hPS: 20.8 kg/mol

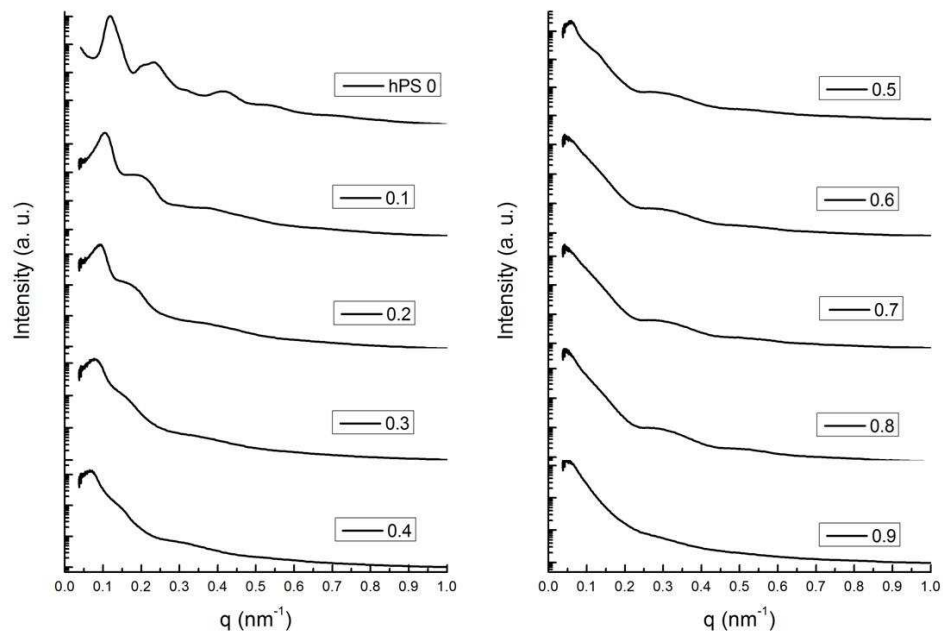


Figure S6. SAXS curves for miktoarm ($f_{PS}=0.37$) and hPS (20.8 kg/mol) blends. The numbers on each curve represent the wt fraction of hPS in each blend.

4. hPS: 44.6 kg/mol

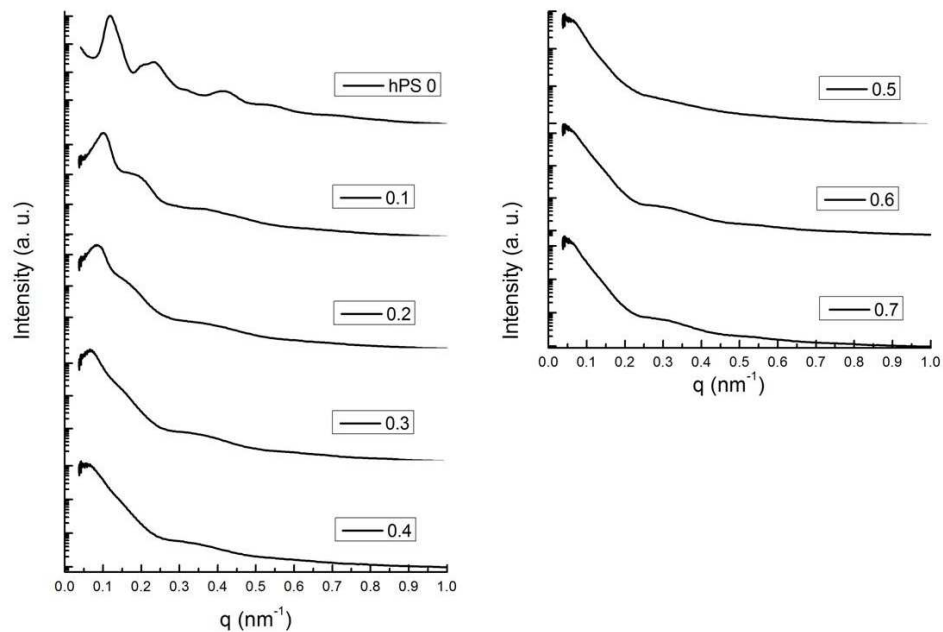


Figure S7. SAXS curves for miktoarm ($f_{PS}=0.37$) and hPS (44.6 kg/mol) blends. The numbers on each curve represent the wt fraction of hPS in each blend.

5. hPS: 79.5 kg/mol

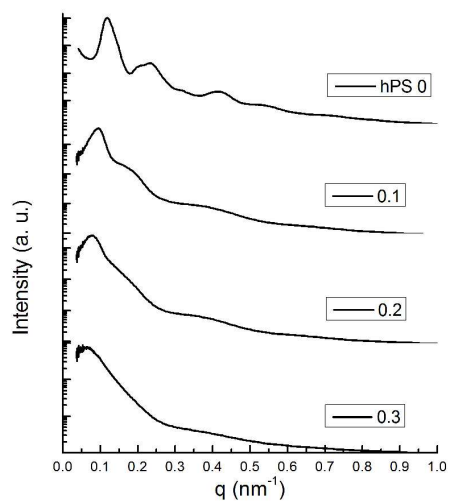


Figure S8. SAXS curves for miktoarm ($f_{PS}=0.37$) and hPS (79.5 kg/mol) blends. The numbers on each curve represent the wt fraction of hPS in each blend.

Part E: Generality of bricks-and-mortar structure

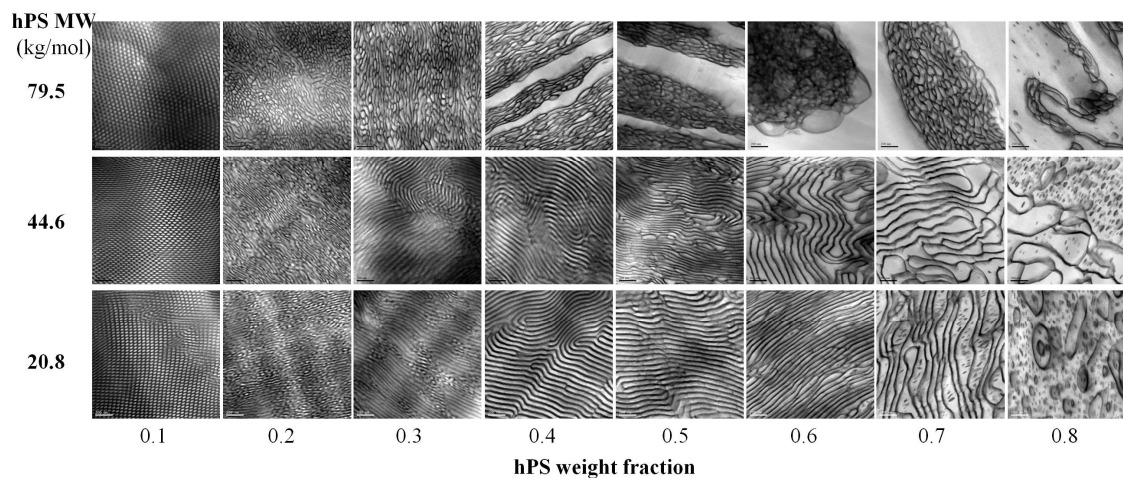


Figure S9. TEM images for miktoarm ($f_{PS}=0.5$) and hPS blends with different compositions. The sample was annealed in high vacuum oven at 150 °C for 2 days. The bricks-and-mortar structures are found only at limited compositions when hPS molecular weight is 79.5 kg/mol. The fluctuation effect is strong above 70 wt% hPS when the molecular weights are 44.6 and 20.8 kg/mol. Notably, the BM phase co-exists with a PS-rich phase after macrophase separation. The scale bars are 200 nm in all images.

Part F: Phase diagram of miktoarm star and hPS by SCFT

SCFT is a mean-field theory lacking thermal fluctuation effects. The SCFT-derived OOTs for miktoarm blends with short hPS polymers were generally consistent with the experimental observations. However, especially for intermediate to large MW hPS, there are several points of inconsistency. The first is that SCFT can only describe ordered mesophases or a structureless disordered phase (DIS). The SCFT phase diagram therefore lacks the BM and micellar phases, both of which are disordered, yet structured. As a consequence, an SCFT-computed boundary from ordered mesophases must terminate in either a two-phase coexistence region with DIS, or a sharp first or second order phase transition to DIS. The experimental results show that when macrophase separation occurs, the BM mesophase co-exists with a hPS-rich structured “emulsion” phase, while SCFT predicts the co-existence of LAM (or HEX) with a hPS-rich structureless DIS phase. Another interesting observation is that SCFT overweights the macrophase separation region of the phase diagram. The computed macrophase separation region is roughly the sum of the BM, macrophase and micelle regions observed experimentally. These findings support the proposition that the BM mesophase (as well as the micellar phase) are created and stabilized by thermal fluctuations, and these phases are coherently minimizing regions of the phase diagram where ordered microphases and macrophase separation would otherwise compete.

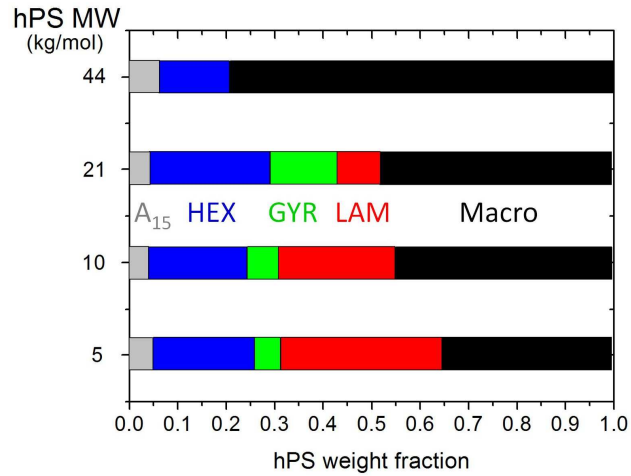


Figure S10. The computed phase diagram of miktoarm ($f_{PS}=0.37$) and hPS by SCFT.

The calculation was carried out at total $\chi \cdot N=150$. A_{15} : the sphere phase with $Pm\bar{3}n$ symmetry; HEX: PS hexagonal cylinder phase with $P6mm$ symmetry; GYR: PS double gyroid phase with $Ia\bar{3}d$ symmetry; LAM: PS and PI lamellar phase; Macro: the macrophase separation between hPS and miktoarm block copolymer. The morphology of neat miktoarm block copolymer is HEX while SCFT predicts A_{15} sphere phase. The inconsistency is due to two factors: 1) f_{PS} locates near the HEX/ A_{15} boundary and there is about 2% uncertainty when determining volume fraction by NMR; 2) the simulation was studied under equal segment length of PS and PI, but actually PI segment length is 1.15 times of PS. The conformational asymmetry shifts the actual phase boundary back to lower f_{PS} .

SCFT method:

The intensive free energies of various phases (lamellar, cylindrical, gyroid, and BCC, FCC, and A_{15} spherical phases) were computed throughout parameter space in order to find the phase boundaries. Each calculation utilized a unit cell, within which the symmetry operations of the relevant phase were enforced and the cell lattice parameter was allowed to relax. Details of the implementation of SCFT can be found elsewhere.[1,2] Additionally, coexistence regions were calculated using the Gibbs Ensemble formalism, wherein chemical and mechanical equilibrium between two separate phases, in two separate cells, are reached via species exchange and volume exchange between the two cells. [3]

Chain block fraction parameters were based on the experimental results.[4] First, the degrees of polymerization N_i were calculated using the block molecular weights. Next, both monomer volumes were rescaled to 0.1 nm^3 , and N_i were scaled accordingly. Now the volume fractions of the various blocks were calculated from the rescaled number fractions. We get 0.250, 0.216, and 0.034, for f_{PS} , f_{PI} , and $f_{PS'}$, respectively. The volume fractions of the homopolymers, as a fraction of the

miktoarm volume, are calculated accordingly. The Flory Huggins parameter (0.049) and statistical segment lengths ($\text{PS}=0.5 \text{ nm}$, $\text{PI}=0.56 \text{ nm}$), with respect to the rescaled monomer volumes, were taken from Balsara. [5] The total interaction strength is $\text{ChiN}=272$. Phase boundaries were calculated at $\text{ChiN}=150$. It was found that higher ChiN had negligible effect on the phase boundaries. 1000 points were used for the miktoarm contour resolution, and up to 128^3 plane waves for the spacial resolution.

- [1] K. T. Delaney, G. H. Fredrickson. *Computer Physics Communications*, 2013, 184, 2102-2110.
- [2] G. H. Fredrickson. *The Equilibrium Theory of Inhomogeneous Polymers*. Oxford: Clarendon, 2006. Print.
- [3] Z. Mester, N. A. Lynd, K. T. Delaney, G. H. Fredrickson. *Macromolecules*, 2014, 47, 1865-1874.
- [4] Weichao Shi, Nathaniel A. Lynd, Damien Montarnal, Yingdong Luo, Glenn H. Fredrickson, Edward J. Kramer, Christos Ntaras, Apostolos Avgeropoulos, Alexander Hexemer *Macromolecules* 2014, 47, 2037–2043
- [5] "Thermodynamics of Polymer Blends", N. P. Balsara and H. B. Eitouni in *Physical Properties of Polymers Handbook*, Second Edition, Chapter 19, p. 339-356, Mark, J.E. (editor), Springer, New York, 2007.

Part G: Monotonic and step-cycle tensile testing results

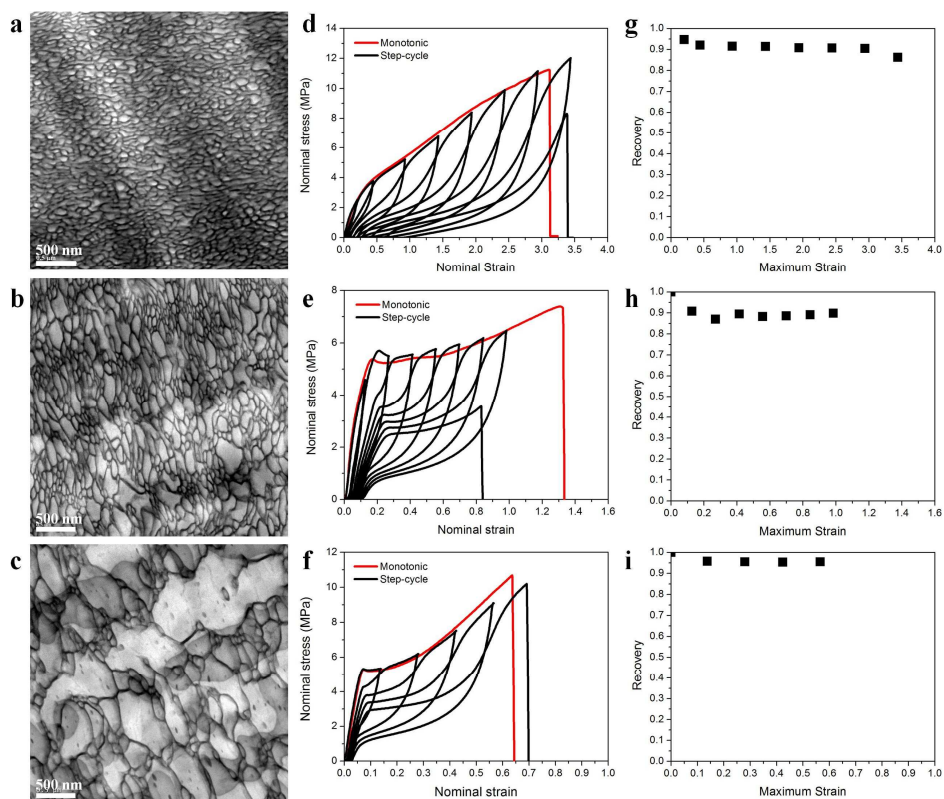


Figure S11. TEM images, monotonic and step-cycle tensile tests and recovery results for mikroarm-hPS blends with 30 wt% (a, d, g), 50 wt% (b, e, h) and 70 wt% (c, f, i) hPS. The mechanical tests include monotonic and step-cycle tensile testing. The recovery of each sample (g, h, i) is calculated from the step-cycle tests.

Part H: Monotonic and modulus at different hPS fractions

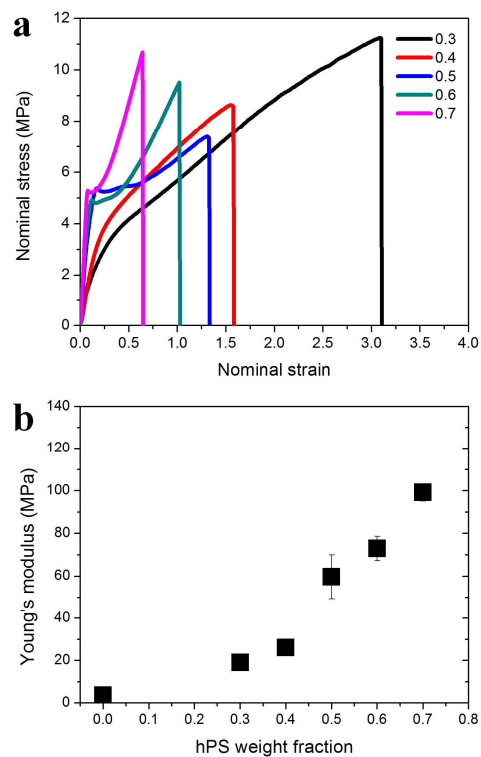


Figure S12. (a) shows the monotonic tensile tests for miktoarm/hPS blends at different hPS weight fractions. (b) is the corresponding Young's modulus at different hPS weight fraction.

Part I: Scattering curves for the tensile-SAXS experiment at different strains

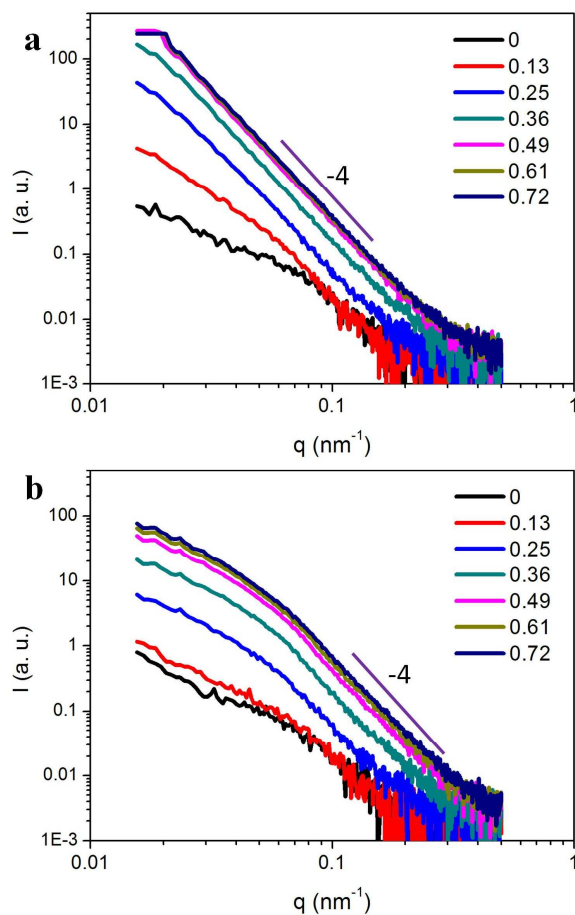


Figure S13. Tensile-SAXS experiments for the miktoarm block copolymer blended with 50 wt% hPS. Images (b) and (c) are scattering curves in the tensile direction and horizontal direction, respectively.